ELSEVIER

Biochimica et Biophysica Acta 1412 (1999) 139–148

BIOCHIMICA ET BIOPHYSICA ACTA
BBA

www.elsevier.com/locate/bba

The mobile loop region of the NAD(H) binding component (dI) of proton-translocating nicotinamide nucleotide transhydrogenase from *Rhodospirillum rubrum*: complete NMR assignment and effects of bound nucleotides

Philip G. Quirk [a,*], K. John Smith [a], Christopher M. Thomas [b], J. Baz Jackson [a]

[a] *School of Biochemistry, University of Birmingham, Edgbaston, Birmingham B15 2TT, UK*
[b] *School of Biological Sciences, University of Birmingham, Birmingham, UK*

Received 15 January 1999; received in revised form 25 March 1999; accepted 3 May 1999

Abstract

The dI component of transhydrogenase binds NAD^+ and NADH. A mobile loop region of dI plays an important role in the nucleotide binding process, and mutations in this region result in impaired hydride transfer in the complete enzyme. We have previously employed one-dimensional ^{1}H-NMR spectroscopy to study wild-type and mutant dI proteins of *Rhodospirillum rubrum* and the effects of nucleotide binding. Here, we utilise two- and three-dimensional NMR experiments to assign the signals from virtually all of the backbone and side-chain protons of the loop residues. The mobile loop region encompasses 17 residues: Asp^{223}-Met^{239}. The assignments also provide a much strengthened basis for interpreting the structural changes occurring upon nucleotide binding, when the loop closes down onto the surface of the protein and loses mobility. The role of the mobile loop region in catalysis is discussed with particular reference to a newly-developed model of the dI protein, based on its homology with alanine dehydrogenase. © 1999 Elsevier Science B.V. All rights reserved.

Keywords: Transhydrogenase; NMR; Nucleotide; Mobile loop region; *Rhodospirillum rubrum*

1. Introduction

The proton-translocating nicotinamide nucleotide transhydrogenase of *Rhodospirillum rubrum* couples the transfer of hydride ions between NAD(H) and NADP(H) to the vectorial pumping of protons across the bacterial cell membrane (for recent reviews see [1–4]), according to the equation:

$$NADH + NADP^+ + H^+_{OUT} \Leftrightarrow$$

$$NAD^+ + NADPH + H^+_{IN}$$

The enzyme has a tripartite structure, comprising regions historically termed domains I, II and III; we now prefer the terms dI, dII and dIII, since the structure of dI is likely to contain two protein domains (P.J. Baker et al., submitted). The dI component binds NAD(H), dIII binds NADP(H), while dII spans the membrane and contains at least part of

Abbreviations: dI.M226F, recombinant dI protein of *R. rubrum* transhydrogenase with Met^{226} replaced by Phe (etc.); DQF-COSY, double quantum filtered correlated spectroscopy; HSQC, heteronuclear single quantum correlation; NMNH, reduced nicotinamide mononucleotide; NOESY, nuclear Overhauser effect spectroscopy

* Corresponding author. Fax: +44-121-414-3982; E-mail: p.g.quirk@bham.ac.uk

0005-2728/99/$ – see front matter © 1999 Elsevier Science B.V. All rights reserved.
PII: S0005-2728(99)00057-2

the proton-translocating machinery. In *R. rubrum*, dI is expressed as a 384 amino acid, 40.3 kDa polypeptide, the product of the *pntAA* gene [5]. During catalysis, hydride ions are transferred directly between nucleotides bound to dI and dIII [6], a reaction that can occur efficiently even in the absence of dII [7,8].

We have previously shown that the dI component of *R. rubrum* contains a protease-sensitive, surface-exposed region, some 20 amino acid residues in length, located towards the middle of the polypeptide chain [9]. As these residues give rise to unusually sharp resonances in the ^{1}H-NMR spectrum, indicating a high degree of segmental mobility, the region was termed the 'mobile loop' [9]. Several site-directed mutant forms of dI, carrying substitutions in the mobile loop region, exhibited severely impaired hydride transfer [10–13]. When nucleotide is bound, the loop residues lose mobility, and are thought to close down onto the surface of the protein. In the bound state, the conformation of the mobile loop allows residues Tyr^{235} and Ala^{236} (invariant in all known dI sequences) to approach within 5–6 Å of the adenosine moiety of bound NADH or 5′-AMP [13,14].

The large size of the dI protein, a dimer of 80.6 kDa total molecular weight [15], has presented difficulties in assigning many of the features of the ^{1}H-NMR spectrum, even though it was apparent that only a small subset of relatively mobile residues contributed significantly to the observed spectrum [9]. These problems were overcome to some extent by the comparison of spectra of the wild-type and mutant dI proteins, but definitive assignment was still possible only for a minority of residues [10,12,13]. A more complete assignment was desirable for (a) the validation of assumptions made during the tentative assignment of signals from one-dimensional spectra, (b) a better delineation of the extent of the mobile loop region, and (c) an improved utilisation of the observed nuclear Overhauser enhancements (NOEs) to yield further structural information on the mobile loop region.

Here, we employ a combination of two- and three-dimensional NMR techniques to assign completely the mobile loop resonances of wild-type dI, and we analyse the effects of nucleotide binding to both wild-type and mutant dI proteins. In examining the structural consequences of nucleotide binding, we refer to a new model of dI (P.J. Baker et al., submitted), developed on the basis of its sequence homology with alanine dehydrogenase [9,15], for which a crystal structure has recently become available [16].

2. Materials and methods

Protocols for the expression and purification of recombinant wild-type and mutant dI proteins have been published [13,17]. Enzymatic properties of the mutant proteins have been reported elsewhere [11–13]. For the production of ^{15}N-labelled dI, the *Nde*I-*Hin*dIII fragment containing the coding sequence was excised from pCD1 and ligated into the corresponding sites of the pET21a vector (Novagen) to produce pPQ1. For expression of isotopically labelled protein, *Escherichia coli* BL21(DE3) containing pPQ1 was grown at 37°C in M9 minimal medium supplemented with 1 g/l $^{15}NH_4Cl$ and 4 g/l glucose, and induced with 1 mM isopropyl β-D-thiogalactopyranoside (IPTG) for 6 h.

NMR spectroscopy was performed using Bruker AMX or Varian UnityPlus spectrometers, operating at 500 MHz and 600 MHz, respectively. Protein samples (0.2–0.5 mM) were dissolved in buffer containing 10 mM $(NH_4)_2SO_4$, 10 mM [$^{2}H_{11}$]Tris, 1 mM dithiothreitol and 0.15% sodium azide, prepared in either 99.9% $^{2}H_2O$ or 8% $^{2}H_2O$/92% $^{1}H_2O$, as required. Several temperatures (20–37°C), pH conditions (pH 6.8–7.6) and NOESY mixing times (100–400 ms) were employed. Standard pulse sequences were used for one-dimensional (pulse-and-collect, Carr-Purcell spin-echo) and two-dimensional (DQF-COSY, NOESY) NMR experiments. The FHSQC [18] and SE-HSQC [19] pulse sequences were utilised in two-dimensional ^{1}H,^{15}N-HSQC and three-dimensional, ^{15}N-resolved NOESY-HSQC experiments. Where appropriate, the water resonance was reduced in size either by presaturation or the WATERGATE gradient technique [20]. HSQC spectra were routinely acquired before and after each NOESY-HSQC experiment; no degradation of the protein was seen, even after 4 days at 20°C. The chemical shifts of ^{1}H resonances were referenced to internal DSS (2,2-dimethyl-2-silapentane-5 sulphonate), and those of ^{15}N resonances were indirectly referenced to DSS.

The dI protein of *R. rubrum* transhydrogenase was modelled onto the crystal structure of alanine dehy-

drogenase from *Phormidium lapideum* [16], using the program Modeller, version 3 [21]. The mobile loop residues, for which there are no corresponding amino acids in alanine dehydrogenase, were inserted between Val^{214} and Glu^{215} of alanine dehydrogenase (taken as equivalent to Ile^{219} and Glu^{242}, respectively, of dI). NAD^+ was inserted, using its coordinates in the alanine dehydrogenase structure, and the model was energy minimised (100 steps, adopted-basis Newton Raphson method). Comparative aspects of the two proteins are discussed in detail elsewhere (P.J. Baker et al., submitted).

3. Results

3.1. Assignment of ^1H and ^{15}N resonances of dI

The large size of the dI dimer is reflected in the observation that only a few, relatively mobile residues produce sharp, well-resolved proton signals in one-dimensional NMR spectra [9]. The 500 MHz ^1H,^{15}N-HSQC spectrum of wild-type dI protein, labelled with ^{15}N, is shown in Fig. 1A. The equivalent spectrum at 600 MHz was virtually identical (not shown). Only 23 out of a possible 364 backbone amide resonances were observed; again an indication that relaxation of most of the protein residues occurs too fast for them to give detectable NMR signals. To assign these resonances, ^{15}N-resolved NOESY-HSQC spectra were acquired for the protein alone, and after the addition of 1.5 mM 5′-AMP. Illustrative portions of the spectrum with 5′-AMP are shown in Fig. 2; 'slices' from the other residues were of comparable quality. Definitive assignment of the mobile loop resonances between Asp^{223} and Met^{239} was possible from the H_i^{α} to H_{i+1}^{N} sequential NOEs observed in these spectra, aided by the H_i^{β} and H_i^{γ} to H_{i+1}^{N} NOEs where the H^{α} signals of successive residues were overlapped. The assignment process was simplified by the almost total absence of longer-range NOEs (see below). Chemical shift values are summarised in Tables 1 and 2. In addition to the mobile loop, a second, highly mobile region of the protein, comprising the sequence -G-Q-G-A-, was assigned to the residues Gly^{381}-Ala^{384}, forming

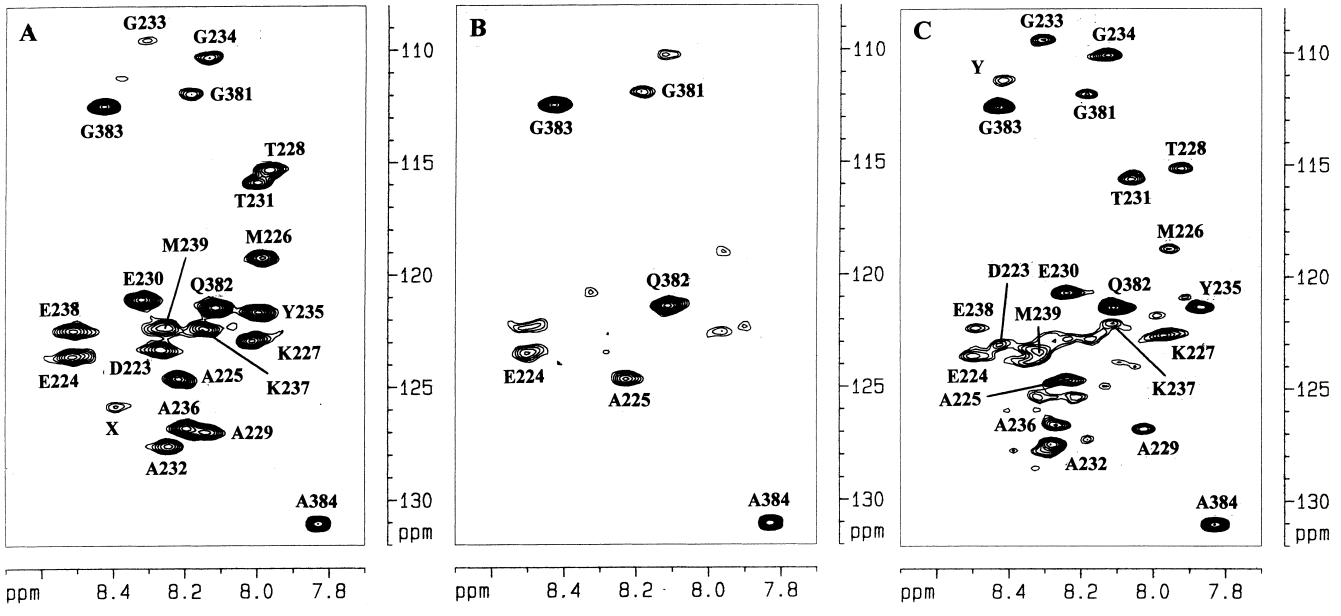

Fig. 1. Part of the 500 MHz ^1H-^{15}N HSQC spectrum of 400 μM wild-type, ^{15}N-labelled dI, showing the backbone amide N-H^N correlations. Two unassigned resonances are indicated by 'X' and 'Y' (see text). A: dI alone. B: As A after addition of 100 μM NADH. Conditions for both experiments were 20°C, 92% H_2O/8% ^2H_2O buffer, pH 7.2. The levels at which the two spectra are plotted were scaled using the Gly^{383} resonance as an internal reference. C: 600 MHz HSQC spectrum of 400 μM wild-type, ^{15}N-labelled dI after addition of 1.5 mM 5′-AMP. Conditions were otherwise identical to those of A and B. The level at which this spectrum was plotted differs from that of spectra A and B, and was chosen to allow all of the signals from the mobile loop residues to be seen.

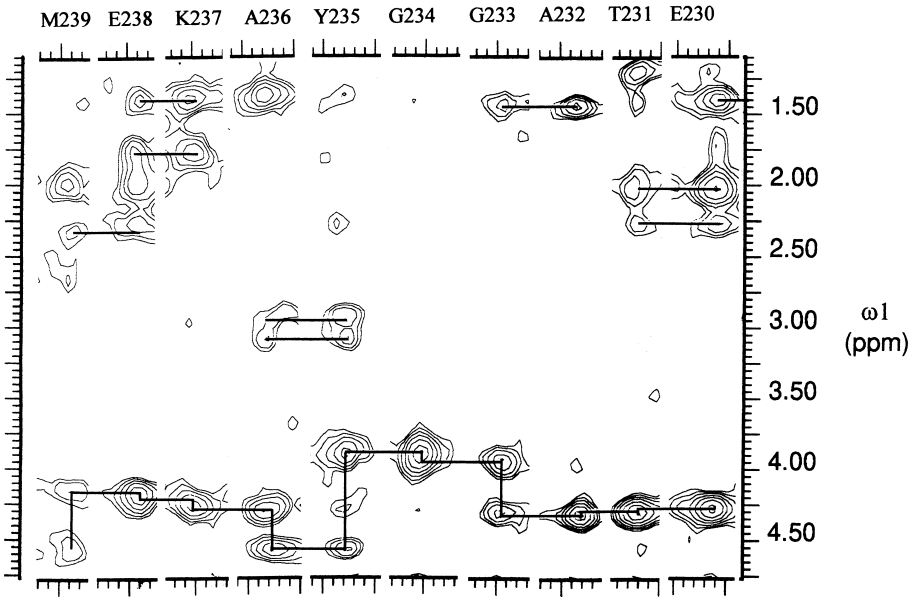

Fig. 2. Series of strips selected from ^{1}H-$^{1}H^{N}$ slices of the 3D ^{1}H-^{15}N NOESY-HSQC spectrum ($^{1}H = 600$ MHz) of 400 μM wild-type, ^{15}N-labelled dI, in the presence of 1.5 mM 5′-AMP. Each vertical strip shows the intra- and inter-residue NOE cross-peaks arising from the H^{N} proton of one residue between Met^{239} and Glu^{230}, as indicated above the strips. The vertical lines connect the H_i^N-H_i^α and H_i^N-H_{i-1}^α cross-peaks of each residue, while the horizontal lines between them connect the H_i^N-H_{i-1}^α and H_{i-1}^N-H_{i-1}^α cross-peaks of adjacent residues. Selected NOEs from side-chain H_i^β and H_i^γ are also indicated by horizontal lines between the H_i^N and H_{i+1}^N cross-peaks of each proton. The H^N and ^{15}N chemical shift values are given in Tables 1 and 2. Conditions were 20°C, 92% H_2O/8% $^{2}H_2O$ buffer, pH 7.2, with a NOESY mixing time of 100 ms. The experiment time was 40 h.

the C-terminal tail of dI. All except two of the backbone amide protons seen in the HSQC spectrum have been assigned. The remaining unidentified signals (marked 'X' and 'Y' in Fig. 1A,C) were weak, and gave no observable NOEs in the three-dimensional NOESY-HSQC spectrum. One of them ('Y', $^{1}H = 8.48$ ppm, $^{15}N = 110.1$ ppm) almost certainly originates from a glycine residue, possibly Gly^{240}.

Further resolution of the side-chain signals from the mobile loop residues was obtained in two-dimensional experiments, making particular use of the intra-residue H^α-H^β and H^α-H^γ proton connectivities. As an example, part of the DQF-COSY spectrum of dI.M226F is shown in Fig. 3. In addition to the five Ala and two Thr resonances, which are particularly well resolved in this mutant, two Lys and at least three Glu/Gln side-chains were observed. Most of these resonances could also be discerned in the DQF-COSY spectrum of wild-type dI (not shown). The COSY spectra again confirm that only a small subset of protein residues relaxes slowly enough to produce observable side-chain connectivities (dI contains a total of 55 Ala, 30 Thr and 27 Lys residues). Further side-chain information was obtained from two-dimensional, 500 MHz ^{1}H-^{1}H NOESY spectra of wild-type and mutant proteins, acquired in $^{2}H_2O$ buffer (Fig. 4).

The $C^\varepsilon H_3$ resonance of the N-terminal methionine residue was identified as the only pH-sensitive singlet signal observed in one-dimensional spectra (not shown) of wild-type dI between pH 7.3 (chemical shift = 1.72 ppm) and pH 8.75 (chemical shift = 1.50 ppm). The upfield shift with increasing pH reflects the deprotonation of the N-terminal amino group; the pK_a was estimated as 8.5 ± 0.1.

In addition to the assignments listed above, prominent signals at 7.32 and 7.19 ppm in the spectrum of wild-type dI have been attributed to the aromatic ring of Phe^{243} on the basis of (a) NOEs to Met^{239} $C^\varepsilon H_3$ (see below), and (b) upfield shifts of these signals in the dI.M226F mutant, relative to wild-type (Table 1). The remaining ^{1}H spectral features which have not been assigned to specific residues include several Asn/Gln side-chain amides, two prominent

Table 1
Assignment of ^{1}H resonances of *R. rubrum* dI

Residue	Chemical shift (ppm)		dI.M226F
	Wild-type	wt+AMP	
Asp^{223} NH	8.35	8.42	
$C^{\alpha}H$	4.57	4.62	
$C^{\beta}H_2$	2.66	2.66	
Glu^{224} NH	8.60	8.59	8.66
$C^{\alpha}H$	4.14	4.15	
$C^{\beta}H_2$	2.03	2.07	
$C^{\gamma}H_2$	2.26	2.28	
Ala^{225} NH	8.31	8.32	8.39
$C^{\alpha}H$	4.19	4.20	4.14
$C^{\beta}H_3$	1.40	1.41	1.24
Met^{226} NH	8.07	8.05	–
$C^{\alpha}H$	4.38	4.35	–
$C^{\beta}H_2$	2.07	2.12	–
$C^{\gamma}H_2$	2.58	2.66	–
$C^{\epsilon}H_3$	2.05	~2.06	–
Phe^{226} NH	–	–	7.92
$C^{\alpha}H$	–	–	4.56
$C^{\beta}H_2$	–	–	3.27, 2.98
ring	–	–	7.31, 7.24
Lys^{227} NH	8.10	8.05	7.95
$C^{\alpha}H$	4.30	4.31	4.30
$C^{\beta}H_2$	1.87	1.88	1.86
$C^{\gamma}H_2$	1.44	1.45	1.44
Thr^{228} NH	8.05	8.01	8.11
$C^{\beta}H$	~4.30	~4.31	4.29
$C^{\gamma}H_3$	1.21	1.21	1.22
Ala^{229} NH	8.22	8.11	8.25
$C^{\alpha}H$	4.30	4.31	4.29
$C^{\beta}H_3$	1.40	1.41	1.40
Glu^{230} NH	8.41	8.33	8.42
$C^{\alpha}H$	4.26	4.28	4.23
$C^{\beta}H_2$	2.03	2.03	2.07, 1.98
$C^{\gamma}H_2$	2.27	2.27	2.25
Thr^{231} NH	8.09	8.15	8.04
$C^{\beta}H$	~4.30	~4.31	4.27
$C^{\gamma}H_3$	1.21	1.21	1.20
Ala^{232} NH	8.33	8.37	8.32
$C^{\alpha}H$	4.34	4.35	4.33
$C^{\beta}H_3$	1.40	1.45	1.42
Gly^{233} NH	8.40	8.39	n.d.
$C^{\alpha}H_2$	n.d.	3.96	n.d.
Gly^{234} NH	8.23	8.21	n.d.
$C^{\alpha}H_2$	3.91	3.92	3.91
Tyr^{235} NH	8.08	7.96	8.07
$C^{\alpha}H$	4.53	4.58	4.53
$C^{\beta}H_2$	3.06, 2.94	3.06, 2.94	3.06, 2.93
ring	7.11, 6.81	7.12, 6.81	7.11, 6.81
Ala^{236} NH	8.29	8.36	8.30
$C^{\alpha}H$	4.26	4.31	4.27
$C^{\beta}H_3$	1.36	1.37	1.37
Lys^{237} NH	8.23	8.20	8.22
$C^{\alpha}H$	4.19	4.27	4.18
$C^{\beta}H_2$	1.79	1.76	1.78
$C^{\gamma}H_2$	1.40	1.37	1.40
Glu^{238} NH	8.59	8.58	8.61
$C^{\alpha}H$	4.15	4.19	4.16
$C^{\beta}H_2$	1.99	2.00	2.01
$C^{\gamma}H_2$	2.27	2.27	2.26
Met^{239} NH	8.36	8.39	n.d.
$C^{\alpha}H$	4.43	4.52	4.43
$C^{\beta}H_2$	1.99	2.04	2.03
$C^{\gamma}H_2$	2.46	n.d.	2.45
$C^{\epsilon}H_3$	1.97	1.86	1.92
Phe^{243} ring	7.32, 7.19	7.30, 7.17	7.31, 7.08
Gly^{381} NH	8.27	8.27	n.d.
$C^{\alpha}H$	4.01	4.01	n.d.
Gln^{382} NH	8.20	8.20	8.20
$C^{\alpha}H$	4.39	4.39	4.39
$C^{\beta}H_2$	2.18, 1.95	2.16, 1.96	2.17, 1.96
$C^{\gamma}H_2$	2.38	2.39	2.38
$CONH_2$	7.61, 6.93	7.61, 6.93	7.61, 6.92
Gly^{383} NH	8.51	8.52	8.51
$C^{\alpha}H_2$	3.95	3.96	3.95
Ala^{384} NH	7.92	7.92	7.91
$C^{\alpha}H$	4.16	4.16	4.16
$C^{\beta}H_3$	1.33	1.33	1.33

Chemical shift values are presented for 20°C and pH 7.2 (wild-type) or pH 6.8 (dI.M226F).
Assignments in other mutants (see also [10,12,13]): dI.K237M, Met^{237} $C^{\alpha}H$ 4.33 ppm, $C^{\beta}H_2$ 2.03 ppm, $C^{\gamma}H_2$ 2.51 ppm, Glu^{238} $C^{\alpha}H$ 4.19 ppm.
n.d., not determined.

Met methyl groups (designated MetB and MetD [10]), and signals with chemical shift values between 1.10 and −0.87 ppm attributable to methyl groups, some of which are ring-shifted by neighbouring aromatic groups.

3.2. Assignment of resonances of mutant dI proteins

Mutations have been made at several positions in the mobile loop region, between residues 226 and 239: dI.M226F, dI.T231C, dI.G234A, dI.Y235F, dI.Y235N, dI.A236G, dI.K237M, dI.M239I and dI.M239F [10,12,13]. The availability of comparable one- and two-dimensional spectra for the wild-type

Table 2
Assignment of ^{15}N resonances of wild-type *R. rubrum* dI

Residue		Chemical shift (ppm)	
		Wild-type	wt+AMP
Asp^{223}		123.2	123.2
Glu^{224}		123.5	123.4
Ala^{225}		124.5	124.5
Met^{226}		119.1	118.7
Lys^{227}		122.8	122.5
Thr^{228}		115.2	115.1
Ala^{229}		126.9	126.7
Glu^{230}		121.0	120.6
Thr^{231}		115.8	115.6
Ala^{232}		127.5	127.4
Gly^{233}		109.4	109.4
Gly^{234}		110.2	110.0
Tyr^{235}		121.6	121.3
Ala^{236}		126.7	126.5
Lys^{237}		122.3	122.0
Glu^{238}		122.4	122.2
Met^{239}		122.2	122.5
Gly^{381}		111.8	111.8
Gln^{382}		121.3	121.3
Gln^{382}	$CONH_2$	114.3	114.2
Gly^{383}		112.4	112.3
Ala^{384}		131.0	131.0

Chemical shift values are presented for 20°C and pH 7.2.

and mutant proteins provided much additional information, confirming the assignments made from the two- and three-dimensional NOESY spectra. For example, the side-chain of Lys^{237} was readily assigned by comparison of the two-dimensional NOESY spectra of wild-type and dI.K237M proteins (Fig. 4), and such mutations often caused small perturbations in the side-chains of residues adjacent to the substitution site, e.g. Glu^{238} H^{α} was shifted downfield in dI.K237M. The $C^{\varepsilon}H_3$ signal of Met^{239} was especially sensitive to changes in neighbouring residues, responding to substitutions at Met^{226}, Gly^{234}, Tyr^{235}, Ala^{236} and Lys^{237}. For comparison with wild-type dI, the partial assignment of dI.M226F is also presented in Table 1. Notable chemical shift changes resulting from the substitution included Ala^{225} $C^{\beta}H_3$ (0.16 ppm upfield), Met^{239} $C^{\varepsilon}H_3$ (0.05 ppm upfield) and the 7.19 ppm component of the Phe^{243} ring (0.11 ppm upfield). Assignments for most of the side-chains introduced by mutation have been reported previously [10,12,13]; those for Met^{237} of dI.K237M are given in the footnote to Table 1.

3.3. Effects of nucleotide binding

We have previously noted that addition of NADH to wild-type dI caused considerable broadening of most of the resolved peaks in the one-dimensional NMR spectrum, along with some shifting of signals, most notably that of the $C^{\varepsilon}H_3$ resonance of Met^{239} [12,14]. Similarly, the addition of 100 μM NADH in the ^{1}H, ^{15}N-HSQC experiment caused extensive broadening of all the signals originating from residues of the mobile loop, while leaving those from the C-terminal tail unaffected (Fig. 1B). This result suggests that the C-terminal tail of dI plays no part in nucleotide binding. The backbone amide proton of Ala^{384} gave a clear doublet in the one-dimensional proton spectrum ($^{3}J_{\alpha N} = 6.9$ Hz), indicating high mobility and consistent with a random backbone conformation. The C-terminal tail may therefore be even less constrained than the mobile loop region, the amide protons of which do not show up clearly in one-dimensional spectra.

When nucleotides with lower binding affinities were substituted for NADH, similar spectral changes resulted, but with substantially less broadening of resonances [14], probably as a result of faster chemical exchange. Thus, virtually all the dI proton signals remained visible in the presence of 1.5 mM 5′-AMP (Fig. 1C), and assignments under these conditions, derived from the NOESY-HSQC spectrum (Fig. 2), are shown in Tables 1 and 2. All but one

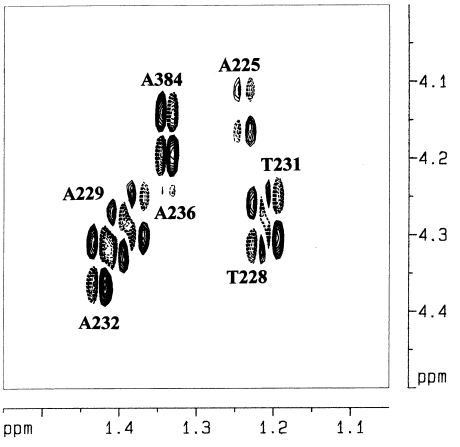

Fig. 3. Part of the 500 MHz DQF-COSY spectrum of 400 μM dI.M226F, showing side-chain connectivities of Ala (H^{α}-H^{β}) and Thr (H^{β}-H^{γ}) residues. Conditions were 37°C, 99.9% $^{2}H_2O$ buffer, $p^{2}H = 7.6$. Positive and negative contours are indicated by continuous and dashed lines, respectively.

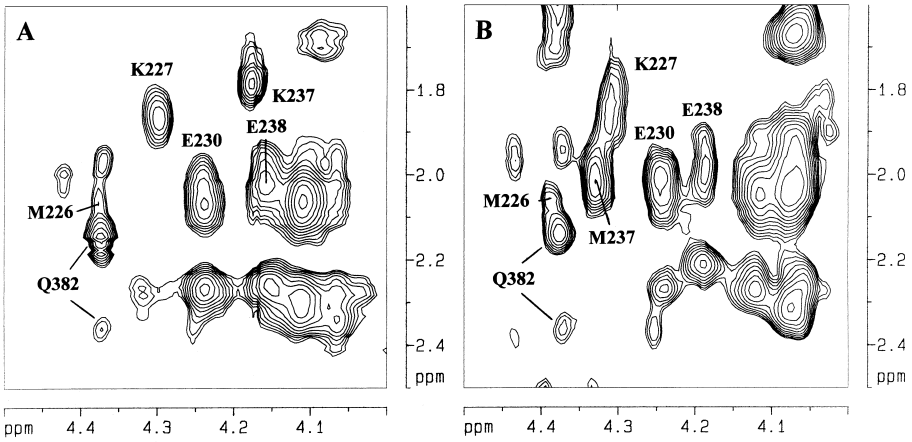

Fig. 4. Part of the 500 MHz ^{1}H-^{1}H NOESY spectra of A: 300 μM wild-type dI; B: 180 μM dI.K237M, showing the assignment of the Lys^{227} and Lys^{237} side-chain protons (H^{α}-H^{β} connectivities). Conditions were 37°C, 99.9% $^{2}H_2O$ buffer, $p^{2}H = 7.6$, with mixing times of 400 ms (wild-type) and 200 ms (dI.K237M). Some additional assignments are indicated.

of the ^{15}N resonances were either unchanged or shifted slightly upfield; the exception was that of Met^{239}, which moved 0.3 ppm downfield. Changes in ^{1}H resonance frequencies were seen for both backbone and side-chain protons, and occurred over the whole of the mobile loop region. These arise from a change in magnetic environment and/or altered rates of chemical exchange, either between dissociable protons and solvent or between 'nucleotide-bound' and 'nucleotide-free' conformations. The largest movements were observed for Ala^{229} H^{N} (0.11 ppm upfield) and Tyr^{235} H^{N} (0.12 ppm upfield), while H^{α} protons undergoing significant resonance shifts included those of Tyr^{235} (0.05 ppm downfield), Lys^{237} (0.08 ppm downfield) and Met^{239} (0.09 ppm downfield). 'Broadening', measured as loss of NH peak height in the HSQC spectrum, occurred with most of the loop residues, but the Gly^{233} resonance became more intense in the presence of 5′-AMP, indicating increased protection from exchange.

3.4. NOE interactions

Inter-residue NOEs in the mobile loop region, assigned from two-dimensional NOESY and three-dimensional NOESY-HSQC experiments, are summarised in Fig. 5. Most were sequential, occurring between residues (*i*, *i*+1), with the only apparent longer-range interactions being between Met^{239} $C^{\varepsilon}H_3$ and two components of an aromatic ring assigned as Phe^{243}. The only other NOEs not expected from a disordered structure were those between Tyr^{235} H^{N} and Ala^{236} (both $C^{\alpha}H$ and $C^{\beta}H_3$), and between Gly^{234} $C^{\alpha}H_2$ and Ala^{236} H^{N}.

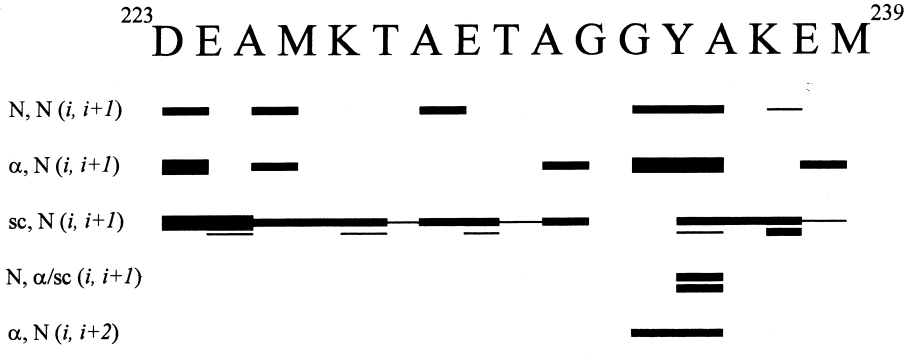

Fig. 5. Inter-residue ^{1}H-^{1}H NOE interactions in the mobile loop region of transhydrogenase, in the presence of 5′-AMP. Data are taken from the 3D NOESY-HSQC experiment (Fig. 4). The thickness of the bars indicates strong (thick), medium (medium) or weak (thin) cross-peak intensities. sc, side-chain protons (H^{β} and beyond).

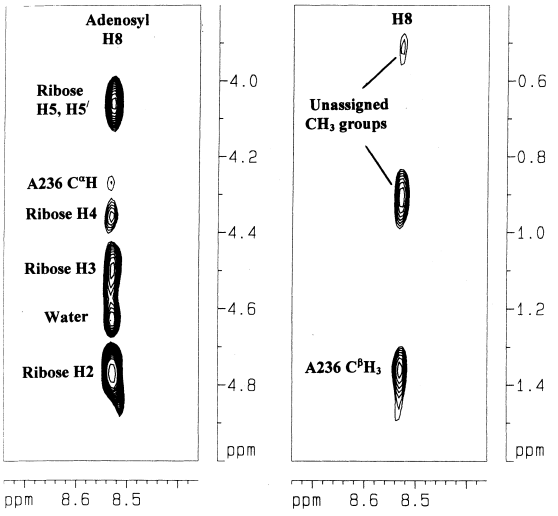

Fig. 6. Two portions of the 500 MHz ^{1}H-^{1}H NOESY spectrum of 400 μM wild-type dI protein, in the presence of 2 mM 5′-AMP. The NOE connectivities from the adenosyl H8 proton are indicated. Conditions were 37°C, 92% H_2O/8% $^{2}H_2O$ buffer, pH 6.8, with a mixing time of 400 ms. The experiment time was 23 h.

The addition of the weakly binding nucleotide 5′-AMP did not result in the appearance of a significant number of new inter-residue NOEs, but caused some increase in intensity of those already present. However, new, intermolecular NOEs between 5′-AMP and dI protein were assigned as follows: adenosyl H8/Tyr^{235} C$^{\alpha}$H (weak intensity), adenosyl H8/Ala^{236} C$^{\alpha}$H (weak), adenosyl H8/Ala^{236} C$^{\beta}$H$_3$ (medium), adenosyl H2/Phe^{243} ring (both components) (very weak), adenosyl H2/Tyr^{235} ring 2,6 (very weak), and ribose H4′/Tyr^{235} ring 2,6 (very weak). Some of these NOEs, including those to Tyr^{235}, were observed at 20°C but not at 37°C. Additional NOEs occurred from the adenosyl H8 and H2 protons to unassigned methyl groups resonating at 0.88 ppm and 0.52 ppm, which must reside outside the mobile loop region of the protein. Part of a NOESY spectrum acquired at 37°C is shown in Fig. 6. A similar pattern of intermolecular NOEs was seen with various combinations of wild-type and mutant proteins, nucleotides (5′-AMP, NADH) and mixing times (100–400 ms), with the notable exception that the adenosyl H8/Ala^{236} C$^{\alpha}$H and C$^{\beta}$H$_3$ interactions were absent when dI.A236G was used [13]. NOE cross-peaks were not observed between backbone amide protons and those of the bound nucleotide.

4. Discussion

The dI protein of *R. rubrum* exists as a dimer in solution, with a total molecular weight of 80.6 kDa [15]. Although this greatly exceeds the size of proteins for which complete assignment and structure determination have been accomplished from NMR data (up to around 30 kDa), the independent, high mobility of the residues of the mobile loop region has allowed identification of virtually all the proton signals from this region. These results have confirmed the origin of all the signals assigned previously from one- and two-dimensional spectra of wild-type and mutant dI proteins [10,12,13]. The only other portion of the backbone showing increased mobility lies at the extreme C-terminal of the protein.

The mobile loop region extends from Asp^{223}-Met^{239}, and includes the GYA motif (Gly^{234}-Ala^{236}), which is invariant in all eleven transhydrogenase sequences published to date. There is no spectroscopic evidence that distinguishes between the two mobile loops present in a dI dimer. The protein binds NADH with a stoichiometry of approximately 1 molecule per dI monomer [22], and this is accompanied by the spectral broadening described previously, with the signals behaving as a single population. We cannot, however, rule out the possibility that the visible resonances arise only from one of the two loop regions, with the residues of the second loop immobilised to the same extent as the rest of the protein, both in the presence and absence of nucleotide.

In the absence of nucleotide, the nuclear Overhauser enhancements arising from the residues of the mobile loop are consistent with a predominantly random-coil conformation. There are too few long-range interactions to define any set of preferred structures, although the NOE pattern of residues Gly^{234}-Ala^{236} is consistent with the existence of a turn in the backbone, even in the absence of bound nucleotide. There are also indications that the mobile loop may have a relatively narrow 'neck', as the mutation of Met^{226} to Phe affects the signals from Tyr^{235}, Met^{239} and Phe^{243} [13]. Similarly, mutations at positions 235 and 239 cause shifts in the signals from Met^{226} and Phe^{243} [10,12], suggesting the proximity of all four residues. Finally, NOEs, albeit very

weak, were observed between the adenosyl H2 proton and the aromatic rings of both Phe[243] and Tyr[235].

The spectral effects following addition of NADH to wild-type dI protein are dominated by broadening, caused by a combination of decreased mobility of the loop residues and an intermediate rate of chemical exchange between nucleotide and protein. The first factor is likely to be the more important, as significant broadening occurs even with signals having little or no chemical shift difference between the free and bound states. To obtain better quality spectra of the bound state, it was necessary to employ nucleotides with lower binding affinity (e.g. 5′-AMP) or loop mutants with lower affinity for nucleotide (e.g. dI.A236G). Several backbone protons are shifted upon addition of nucleotide, but it is not possible to draw a direct correlation between a change in chemical shift and a change in conformation. The intensities of the long-range Met[239]-Phe[243] NOEs are unaltered by the presence of nucleotide, suggesting that the relative organisation of the two side-chains is unchanged. Although the loop residues may adopt a more structured conformation in the presence of nucleotide, the relaxation properties of this state may make any additional NOE interactions difficult to detect.

Although the dI protein can distinguish between NAD^+ ($K_d > 300$ μM) and NADH ($K_d = 30$ μM), the only detectable protein-nucleotide interactions involve the adenosine moiety and residues Tyr[235] and Ala[236] of the mobile loop, and the side-chain of Phe[243]. While this finding provides a convincing explanation for the conservation of the GYA motif, there must be additional protein-nucleotide interactions, undetectable by NMR spectroscopy, involving the nicotinamide moiety.

In the model of dI (Fig. 7), the mobile loop region is shown extended away from the rest of the protein. Although the location of the base of the loop is not certain, due to limited sequence identity between the two proteins in the preceding region, it is clear that the length of the mobile portion of backbone is sufficient to allow the side-chains of Tyr[235] and Ala[236] to take up a position close to the adenine ring of the bound NAD^+, consistent with the observed NOE interactions. In alanine dehydrogenase, the second substrate, alanine, binds on the opposite side of the cleft between the two domains, and a conformational

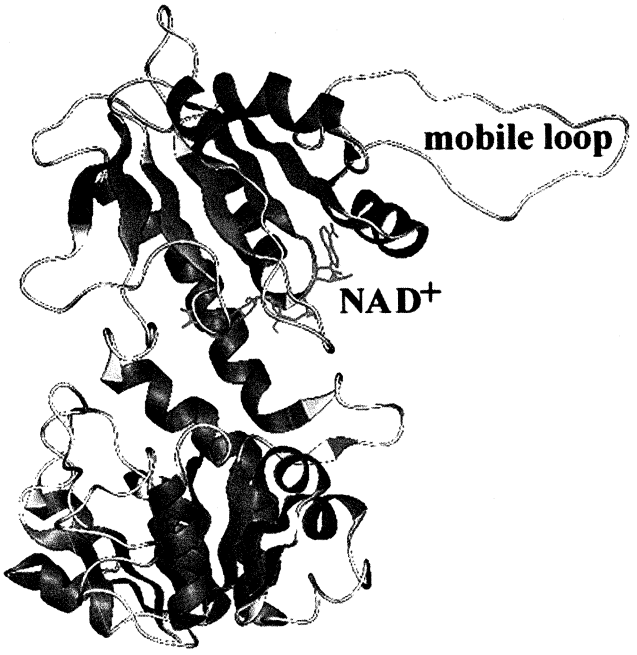

Fig. 7. Molecular model of the dI protein of *R. rubrum*, derived from the crystal structure of alanine dehydrogenase. Predicted α-helices and β-strands are indicated, along with the position of bound NAD^+. The mobile loop is shown extended outwards from the surface of the protein.

change is believed to bring the two substrates into close enough proximity to react with each other [16]. With transhydrogenase, however, the second substrate, NADP(H), is presented to dI.NAD(H) tightly bound to the 20 kDa dIII component, and the question arises as to how the substrates are brought together in order to allow direct hydride transfer to occur. While a complete description of the interactions between dI and dIII must await further experimental investigation, one possibility is that in the dI-dIII complex, NADP(H) bound to dIII takes up a location towards the back of the cleft of dI (towards the left of Fig. 7), with its nicotinamide ring facing that of NAD(H). The role of the mobile loop could be to help in this positioning process. The rate of hydride transfer will be critically dependent on the distance between the C4 atoms of the two nicotinamide rings and their relative orientation. By modulating these parameters, conformational changes in the loop might restrict hydride transfer in the 'open' state of the enzyme and favour the reaction in the 'occluded' state (see [1]). It is noteworthy that the nucleotide analogue NMNH, lacking the adeno-

sine moiety but containing the reduced nicotinamide ring as found in NADH, binds only very weakly to dI [14,23] and is a very poor competitive inhibitor of transhydrogenation [23]; interaction between the adenosine moiety and the mobile loop residues appears to be a prerequisite for binding of the nicotinamide moiety. We have described some of the interactions between nucleotide and loop which may play important roles in the binding process.

Acknowledgements

We are very grateful to Prof. David Rice and Dr. Pat Baker, University of Sheffield, for providing us with the coordinates of the X-ray structure of alanine dehydrogenase. We thank Drs. Barry Levine, Eva Hyde, Mark Jeeves and Jamie Venning for many helpful discussions, and Tony Pemberton for skilled maintenance of the NMR spectrometers. This research was supported by a grant from the Wellcome Trust. This is a contribution from the Birmingham Biological NMR Unit, also funded by the Wellcome Trust.

References

[1] J.B. Jackson, P.G. Quirk, N.P.J. Cotton, J.D. Venning, S. Gupta, T. Bizouarn, S.J. Peake, C.M. Thomas, Biochim. Biophys. Acta 1365 (1998) 79–86.
[2] P.D. Bragg, Biochim. Biophys. Acta 1365 (1998) 98–104.
[3] Y. Hatefi, M. Yamaguchi, FASEB J. 10 (1996) 444–452.
[4] J. Rydström, X. Hu, O. Fjellström, J. Meuller, J. Zhang, C. Johansson, T. Bizouarn, Biochim. Biophys. Acta 1365 (1998) 10–16.
[5] R. Williams, N.P.J. Cotton, C.M. Thomas, J.B. Jackson, Microbiology 140 (1994) 1595–1604.
[6] J.D. Venning, R.L. Grimley, T. Bizouarn, N.P.J. Cotton, J.B. Jackson, J. Biol. Chem. 272 (1997) 27535–27538.
[7] M. Yamaguchi, Y. Hatefi, J. Biol. Chem. 270 (1995) 28165–28168.
[8] C. Diggle, T. Bizouarn, N.P.J. Cotton, J.B. Jackson, Eur. J. Biochem. 241 (1996) 162–170.
[9] C. Diggle, N.P.J. Cotton, R.L. Grimley, P.G. Quirk, C.M. Thomas, J.B. Jackson, Eur. J. Biochem. 232 (1995) 315–326.
[10] C. Diggle, P.G. Quirk, T. Bizouarn, R.L. Grimley, N.P.J. Cotton, C.M. Thomas, J.B. Jackson, J. Biol. Chem. 271 (1996) 10109–10115.
[11] T. Bizouarn, R. Grimley, C. Diggle, C.M. Thomas, J.B. Jackson, Biochim. Biophys. Acta 1320 (1997) 265–274.
[12] R.L. Grimley, P.G. Quirk, T. Bizouarn, C.M. Thomas, J.B. Jackson, Biochemistry 36 (1997) 14762–14770.
[13] S. Gupta, P.G. Quirk, J.D. Venning, J. Slade, T. Bizouarn, R.L. Grimley, N.P.J. Cotton, J.B. Jackson, Biochim. Biophys. Acta 1409 (1998) 25–38.
[14] T. Bizouarn, C. Diggle, P.G. Quirk, R.L. Grimley, N.P.J. Cotton, C.M. Thomas, J.B. Jackson, J. Biol. Chem. 271 (1996) 10103–10108.
[15] I.J. Cunningham, R. Williams, T. Palmer, C.M. Thomas, J.B. Jackson, Biochim. Biophys. Acta 1100 (1992) 332–338.
[16] P.J. Baker, Y. Sawa, H. Shibata, S.E. Sedelnikova, D.W. Rice, Nature Struct. Biol. 5 (1998) 561–567.
[17] C. Diggle, M. Hutton, G.R. Jones, C.M. Thomas, J.B. Jackson, Eur. J. Biochem. 228 (1995) 719–726.
[18] S. Mori, C. Abeyguanawardana, M.O. Johnson, P. Vanzyl, J. Magn. Reson. b 108 (1995) 94–98.
[19] O.W. Zhang, L.E. Kay, J.P. Olivier, J.D. Formankay, J. Biol. NMR 4 (1994) 845–858.
[20] V. Saudek, M. Piotto, V. Sklenár, Bruker Rep. 140 (1994) 6–9.
[21] A. Šali, T.L. Blundell, J. Mol. Biol. 234 (1993) 779–815.
[22] T. Bizouarn, C. Diggle, J.B. Jackson, Eur. J. Biochem. 239 (1996) 737–741.
[23] X. Hu, PhD. Thesis, Göteborg University, Göteborg, Sweden, 1998.